

# $|V_{ub}|$ from Exclusive Semileptonic $B \rightarrow \pi$ Decays

Jonathan M Flynn<sup>a</sup> and Juan Nieves<sup>b</sup>

<sup>a</sup>School of Physics and Astronomy, University of Southampton  
Highfield, Southampton SO17 1BJ, UK

<sup>b</sup>Departamento de Física Atómica, Molecular y Nuclear, Universidad de Granada,  
E-18071 Granada, Spain

## Abstract

We use Omnès representations of the form factors  $f_+$  and  $f_0$  for exclusive semileptonic  $B \rightarrow \pi$  decays, paying special attention to the treatment of the  $B^*$  pole and its effect on  $f_+$ . We apply them to combine experimental partial branching fraction information with theoretical calculations of both form factors to extract  $|V_{ub}|$ . The precision we achieve is competitive with the inclusive determination and we do not find a significant discrepancy between our result,  $|V_{ub}| = (3.90 \pm 0.32 \pm 0.18) \times 10^{-3}$ , and the inclusive world average value,  $(4.45 \pm 0.20 \pm 0.26) \times 10^{-3}$  [1].

## 1 Introduction

The magnitude of the Cabibbo-Kobayashi-Maskawa matrix element  $V_{ub}$  can be determined from both inclusive and exclusive semileptonic  $B$  meson decays. There has been a recent dramatic improvement in the quality of the experimental data for the exclusive decays [2–6], coupled with the appearance of the first dynamical lattice QCD and improved lightcone sumrule calculations of the relevant form factors [7–12]. Dispersive approaches were combined with lattice results in [13] and with leading order heavy meson chiral perturbation theory and perturbative QCD inputs in [14]. The appearance of the first partial branching fraction measurements for  $B \rightarrow \pi l \nu$  [2] made it possible [15] to combine dispersive constraints with experimental differential decay rate information and theoretical calculations of both form factors in limited regions of  $q^2$  in order to improve the determination of  $|V_{ub}|$ . In [16] it was shown that the quality of the inputs now makes it possible for the exclusive determination to compete in precision with the inclusive one<sup>1</sup>. Thus the compatibility of the two determinations becomes an interesting issue.

To perform the exclusive  $|V_{ub}|$  extraction one needs a model-independent parametrisation of the form factors. In [16] a parametrisation inspired by dispersive bounds calculations was used. An alternative simple parametrisation using a multiply-subtracted Omnès representation for  $f_+$ , based on unitarity and analyticity properties, was employed in [18]. A shortcoming in the treatment of the  $B^*$  was pointed out in [19]. In this letter we have addressed this by improving the treatment of the  $B^*$  within the Omnès framework. We have also incorporated the scalar form factor  $f_0$  in a simultaneous analysis and examined the possible effects of correlations among lattice inputs. Finally, we have taken advantage of new experimental data from the BaBar 12-bin untagged analysis [6].

The outcome is that the precision achieved for  $|V_{ub}|$  is indeed competitive with the inclusive determination and that we do not find a significant discrepancy between our result,  $|V_{ub}| = (3.90 \pm 0.32 \pm 0.18) \times 10^{-3}$ , and the inclusive world average value,  $(4.45 \pm 0.20 \pm 0.26) \times 10^{-3}$  [1].

<sup>1</sup>See [17] for updates of the fits in [16].

## 2 Omnès Parametrisations

In our previous work [18, 20] with the Omnès parametrisation [21, 22] for the form factor  $f_+(q^2)$ , we treated the  $B^*$  as a bound state and took the  $B\pi$  elastic scattering phase shift to be  $\pi$  at threshold,  $s_{\text{th}} = (m_B + m_\pi)^2$ . By using multiple subtractions and approximating the phase shift by  $\pi$  from  $s_{\text{th}}$  to infinity, this led to a parametrisation:

$$f_+(q^2) = \frac{1}{s_{\text{th}} - q^2} \prod_{i=0}^n [f_+(s_i)(s_{\text{th}} - s_i)]^{\alpha_i(q^2)}, \quad (1)$$

with  $n + 1$  subtractions at  $q^2 \in \{s_0, s_1, \dots, s_n\}$ , below threshold (the  $\alpha_i(q^2)$  are defined in equation (6) below). This parametrisation requires as input only the form factor values  $\{f_+(q_i^2)\}$  at  $n + 1$  positions  $q_i^2$ .

Using this parametrisation in a combined fit to experimental data and theoretical form-factor calculations (lattice QCD and lightcone sumrules) allows an extraction of  $|V_{ub}|$  with precision competitive to the inclusive determination. This parametrisation and others were compared in reference [19] where the form factor  $f_+$  was determined by fitting BaBar experimental partial branching fraction data in 12 bins [5, 23] and using  $|V_{ub}|$  determined from Unitarity Triangle fits. Good agreement was found between the Omnès parametrisation of equation (1) and parametrisations using

$$f_+(q^2) = \frac{1}{P(q^2)\phi(q^2, t_0)} \sum_{n=0}^{\infty} a_n z(q^2, t_0)^n \quad (2)$$

for two choices of  $t_0$ . The coefficients  $a_n$  satisfy the dispersive constraint  $\sum_n a_n^2 \leq 1$  [16]. Expressions for  $P$  and  $\phi$  can be found in [16]. When we use the parametrisation in equation (2), we will set  $t_0 = s_{\text{th}}(1 - \sqrt{1 - q_{\text{max}}^2/s_{\text{th}}})$ , which is the ‘preferred choice’, labelled BGLa, in [19] (this choice for  $t_0$  ensures that  $|z| \leq 0.3$  for  $0 \leq q^2 \leq q_{\text{max}}^2$ ). We will refer to the parametrisation using this functional form as the  $z$ -expansion or ZE below.

Fits for  $f_+(q^2)$  using the Omnès and ZE parametrisations deviated from each other by a few per cent only in the largest  $q^2$  region, close to  $q_{\text{max}}^2$ , which has little influence on the decay width and  $|V_{ub}|$  (see figure 2 in [19]). This is also the region where there is no theoretical information on the form factors. In figure 1 we show a similar comparison, including bands showing statistical fluctuations arising from the fits. We have fitted the same dataset as in [18], but replacing the 5-bin BaBar untagged analysis [4] with the updated 12-bin results from [6]. The ZE fit has been performed truncating the power series in equation (2) at  $n = 2$ , for comparison with figure 2 in [19], or  $n = 3$ , so that all fits have the same number of parameters. The green dashed lines show the Omnès fit using equation (1). The plot shows that once fluctuations are taken into account the differences are not significant.

Nevertheless, we show here that by treating the  $B^*$  explicitly as a pole of the form factor, we can understand and reduce the small deviation in the central fits at large  $q^2$ . This is illustrated by the solid blue lines in figure 1. We achieve this without altering the main results obtained for  $|V_{ub}|$  and  $f_+$  in the  $q^2$  region where theoretically calculated values lie. The new parametrisation, shown below in equation (7), is obtained from equation (1) by replacing  $s_{\text{th}}$  with  $m_{B^*}^2$ . As before, the parametrisation relies only on very general properties of analyticity and unitarity and so, although simple, is well-founded.

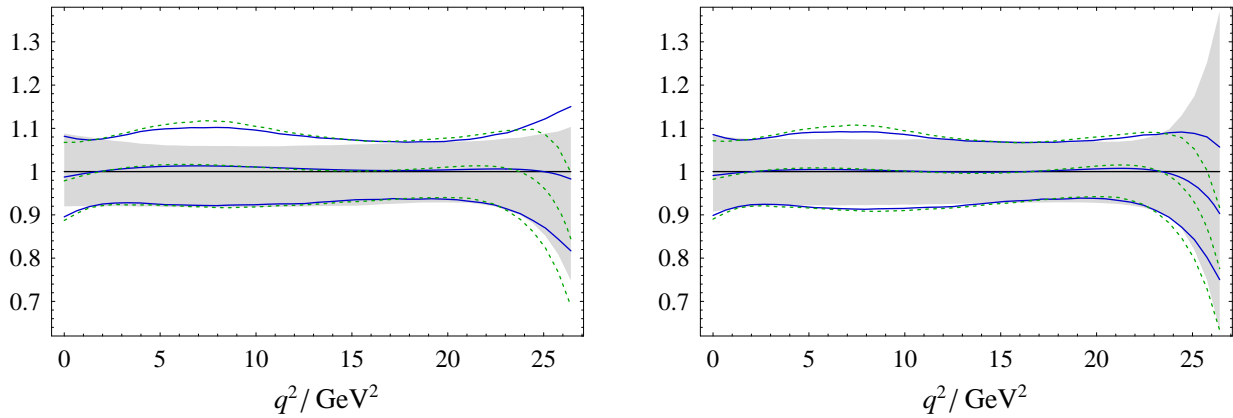


**Figure 1** Comparison of fits to  $f_+(q^2)$  using Omnès or ZE parametrisations. Each fit is plotted with its own error bands, but normalised by the central fit for the ZE. Thus, the horizontal line at 1 and the grey band show the ZE fit with its 68% statistical error band, the solid blue lines indicate the Omnès fit of equation (7) and the green dashed lines show the Omnès fit of equation (1). The left-hand plot uses a ZE fit with three parameters and thus can be compared to figure 2 in [19], while the right-hand plot uses a four-parameter ZE fit. All Omnès fits use four parameters (four subtraction points).

To obtain the new parametrisation we observe that, if  $f_+(q^2)$  has a pole at  $q^2 = m_{B^*}^2$ , then  $\mathcal{F}(q^2) \equiv (m_{B^*}^2 - q^2)f_+(q^2)$  has no poles and satisfies

$$\frac{\mathcal{F}(s + i\epsilon)}{\mathcal{F}(s - i\epsilon)} = \exp(2i\delta_{1/2,1}(s)), \quad s \geq s_{\text{th}} \quad (3)$$

where  $\delta_{IJ}$  is the phase-shift for elastic  $\pi B \rightarrow \pi B$  scattering in the isospin  $I$  and total angular momentum  $J$  channel. This is because  $f_+$  satisfies a similar equation as required by Watson's theorem [24] and we have multiplied it by a real function. An  $(n+1)$ -subtracted Omnès representation can now be written for  $\mathcal{F}(q^2)$ , with  $q^2 < s_{\text{th}}$ , which reads:

$$\mathcal{F}(q^2) = \left( \prod_{i=0}^n [\mathcal{F}(s_i)]^{\alpha_i(q^2)} \right) \exp \left\{ I_{\delta}(q^2; s_0, \dots, s_n) \prod_{j=0}^n (q^2 - s_j) \right\}, \quad (4)$$

$$I_{\delta}(q^2; s_0, \dots, s_n) = \frac{1}{\pi} \int_{s_{\text{th}}}^{+\infty} \frac{ds}{(s - s_0) \cdots (s - s_n)} \frac{\delta_{1/2,1}(s)}{s - q^2}, \quad (5)$$

$$\alpha_i(s) \equiv \prod_{j=0, j \neq i}^n \frac{s - s_j}{s_i - s_j}, \quad \alpha_i(s_j) = \delta_{ij}, \quad \sum_{i=0}^n \alpha_i(s) = 1. \quad (6)$$

This representation requires as input the phase shift  $\delta_{1/2,1}(s)$  plus the values  $\{\mathcal{F}(s_i)\}$  at  $n+1$  positions  $\{s_i\}$  below the  $\pi B$  threshold. For sufficiently many subtractions, we can approximate  $\delta_{1/2,1}(s)$  by zero above threshold (see appendix A). In this case we obtain,

$$f_+(q^2) = \frac{1}{m_{B^*}^2 - q^2} \prod_{i=0}^n [f_+(s_i)(m_{B^*}^2 - s_i)]^{\alpha_i(q^2)}. \quad (7)$$

This amounts to finding an interpolating polynomial for  $\ln \mathcal{F}(q^2) = \ln[(m_{B^*}^2 - q^2)f_+(q^2)]$  passing through the points  $\mathcal{F}(s_i) = (m_{B^*}^2 - s_i)f_+(s_i)$ . Similarly, our earlier parametrisation in equation (1) used an interpolating polynomial for  $\ln[(s_{\text{th}} - q^2)f_+(q^2)]$ . While one could always propose

a parametrisation using an interpolating polynomial for  $\ln[g(q^2)f_+(q^2)]$  for a suitable function  $g(q^2)$ , the derivation using the Omnès representation shows that taking  $g(q^2) = m_{B^*}^2 - q^2$  (and equally  $s_{\text{th}} - q^2$ ) is physically motivated. From here onwards we will use equation (7) as our preferred parametrisation for  $f_+$ .

When using our parametrisation in the extraction of  $|V_{ub}|$ , we make 4 subtractions. This is sufficient to justify using no information about the phase shift beyond its value at  $s_{\text{th}}$ . To check this, we have put in a model for the  $B\pi$  phase shift [20] and confirmed that induced changes in our results are much smaller than the fluctuations produced by the errors in our inputs. This can be understood because with four evenly-spaced subtractions at  $\{0, 1/3, 2/3, 1\}q_{\text{max}}^2$ , the factor  $\exp[I_{\delta} \times \prod_{j=0}^n (q^2 - s_j)]$  in equation (4) given by this model deviates from unity by no more than  $6 \times 10^{-4}$  for  $0 \leq q^2 \leq q_{\text{max}}^2$  (and, of course, is unity at each subtraction point).

Since  $f_+$  and the scalar form factor  $f_0$  satisfy the constraint  $f_+(0) = f_0(0)$  we will combine theoretical inputs for  $f_+$  and  $f_0$  with experimental  $B \rightarrow \pi l \nu$  partial branching fraction information to check the effect on the extracted value of  $|V_{ub}|$ . We will investigate the effect of using the  $f_+$  information alone or using both form factors.

For the scalar form factor  $f_0$  there is no pole below threshold, so that we will use an Omnès formula like equation (4) for  $f_0(q^2)$ , with  $\mathcal{F} \rightarrow f_0$  and  $\delta_{1/2,1} \rightarrow \delta_{1/2,0}$ . For sufficiently many subtractions, we can approximate  $\delta_{1/2,0}$  by zero above threshold. Our recent analysis of the scalar form factor [25] for  $B \rightarrow \pi$  decays suggested the existence of a resonance with mass around 5.6 GeV. This could be incorporated in an Omnès parametrisation like that of equation (7), but (as we have confirmed) has negligible effect on  $|V_{ub}|$  and  $f_+$  in our fit, producing only a small increase of around 7% in the value of  $f_0$  close to  $q_{\text{max}}^2$ .

### 3 Application to $|V_{ub}|$

We have used experimental data for the partial branching fractions of  $B \rightarrow \pi l \nu$  decays in  $q^2$  bins from both tagged and untagged analyses. The tagged analyses from CLEO [2], Belle [3] and BaBar [5] use three bins, while BaBar's untagged analysis [6] uses twelve. CLEO and BaBar combine results for neutral and charged  $B$ -meson decays using isospin symmetry, while Belle quote separate values for  $B^0 \rightarrow \pi^- l^+ \nu_l$  and  $B^+ \rightarrow \pi^0 l^+ \nu_l$ . For our analysis, for the three-bin data, we have combined the Belle charged and neutral  $B$ -meson results and subsequently combined these with the CLEO and BaBar results. The resulting input values can be found in table II of [18]. Since the systematic errors of the three-bin data are small compared to the statistical ones, we have ignored correlations in the systematic errors and combined errors in quadrature. For the 12-bin BaBar data [6], complete correlation matrices are available in the EPAPS database [26] for both statistical and systematic errors and we have used these in our fits (we used the results corrected for final state radiation effects). We have assumed no correlation between the untagged and the tagged analyses.

When computing partial branching fractions, we have used  $\tau_{B^0} = 1/\Gamma_{\text{Tot}} = (1.527 \pm 0.008) \times 10^{-12}$  s [1] for the  $B^0$  lifetime.

Since the effects of finite electron and muon masses are beyond current measurement precision, the experimental results provide information on the  $q^2$  shape of  $f_+$ . Theoretical calculations provide information on  $f_+$  and  $f_0$ .

We use the lightcone sumrule (LCSR) result  $f_+(0) = f_0(0) = 0.258 \pm 0.031$  [12] and lattice QCD results from dynamical simulations at larger  $q^2$  from HPQCD [7] and FNAL-MILC [8–11]. The

FNAL-MILC results [8–11] are still preliminary. Therefore we use the three  $f_+(q^2)$  values quoted in [16] and read off three values for  $f_0(q^2)$  at the same  $q^2$  points from [9]. These are

$$\begin{aligned} f_0(15.87 \text{ GeV}^2) &= 0.425 \pm 0.033 \\ f_0(18.58 \text{ GeV}^2) &= 0.506 \pm 0.037 \\ f_0(24.09 \text{ GeV}^2) &= 0.800 \pm 0.067 \end{aligned} \tag{8}$$

The errors shown are statistical. A further 11% systematic error should be added.

We implement the fitting procedure described in [18] using four evenly-spaced Omnès subtraction points at  $\{0, 1/3, 2/3, 1\}q_{\text{max}}^2$  (with  $\chi$ -squared function given in equation (10) of [18]), with the obvious changes to incorporate  $f_0$ . As before, we have assumed that the lattice input form factor data have independent statistical uncertainties and fully-correlated systematic errors. We have not assumed correlations between results for  $f_+$  and  $f_0$ , though we will comment further on this below. Furthermore, we ignore possible correlations between the HPQCD and FNAL-MILC lattice inputs. These correlations are unknown and we showed in [18] that unless they are very strong they will have little effect on  $|V_{ub}|$ .

The best-fit parameters are

$$\begin{aligned} |V_{ub}| &= (3.90 \pm 0.32) \times 10^{-3} \\ f_+(0) = f_0(0) &= 0.226 \pm 0.022 \\ f_+(q_{\text{max}}^2/3) &= 0.417 \pm 0.039 \\ f_+(2q_{\text{max}}^2/3) &= 0.941 \pm 0.064 \\ f_+(q_{\text{max}}^2) &= 7.29 \pm 1.28 \\ f_0(q_{\text{max}}^2/3) &= 0.342 \pm 0.053 \\ f_0(2q_{\text{max}}^2/3) &= 0.508 \pm 0.040 \\ f_0(q_{\text{max}}^2) &= 1.09 \pm 0.21 \end{aligned} \tag{9}$$

The fit has  $\chi^2/\text{dof} = 0.62$  for 28 degrees of freedom, while the Gaussian correlation matrix can be found in appendix B.

In figure 2 we show the fitted form factors, the differential decay rate calculated from our fit and the quantities  $\log[(m_{B^*}^2 - q^2)f_+(q^2)/m_{B^*}^2]$  and  $P\phi f_+$  where the details of the fit and inputs can better be seen. The dashed magenta curve in the  $P\phi f_+$  plot is a cubic polynomial fit in  $z$  to the output from our analysis. We note that the sum of squares of the coefficients in this polynomial safely satisfies the dispersive constraint  $\sum_n a_n^2 \leq 1$  [16].

Compared to our previous results [18] we find that the central value of  $|V_{ub}|$  decreases by 3% compared with an error of around 8%. Similarly, the central values of  $f_+(0)$  and  $f_+(q_{\text{max}}^2)$  move up by around half their errors, while  $f_+(q_{\text{max}}^2/3)$  increases by an amount comparable with its error. At  $2q_{\text{max}}^2/3$ , in the neighbourhood of which most of the form factor data is concentrated, there is hardly any change. The result for  $f_0(q_{\text{max}}^2)$  agrees with that obtained in our recent analysis of the scalar form factor alone [25]. We make some remarks on these results:

- We have checked that the changes in the results for  $f_+(0)$ ,  $f_+(q_{\text{max}}^2/3)$  and  $|V_{ub}|$  stem from using the updated BaBar untagged data.
- We have checked that the change in  $f_+(q_{\text{max}}^2)$ , which has little effect on the shape of the form factor in the  $q^2$  range where experimental and theoretical information exists, arises from our use of the new Omnès parametrisation of equation (7) and reflects the existence of a pole in  $f_+$  at  $q^2 = m_{B^*}^2$ .

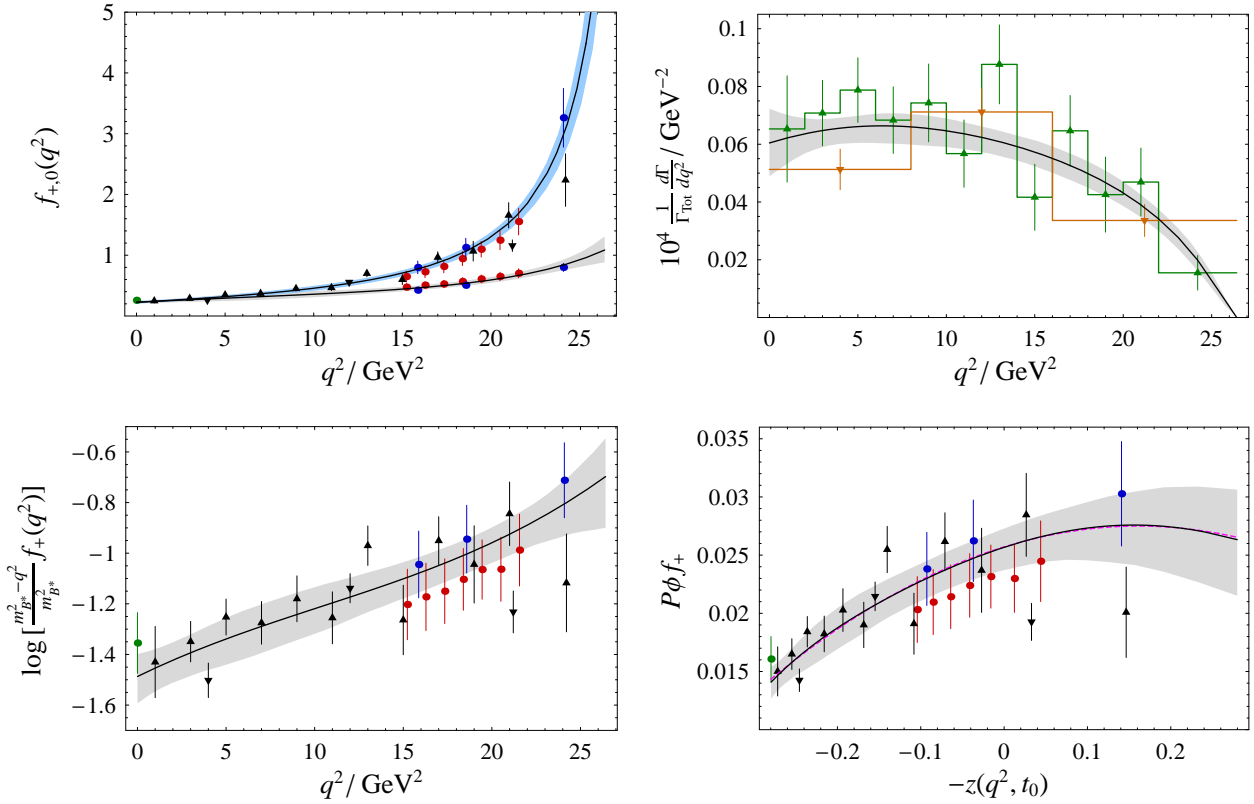


**Figure 2** Results obtained from the fit to experimental partial branching fraction data and theoretical form factor calculations. The top left plot shows the two form factors with their error bands, the lattice and LCSR input points (dots: green LCSR, red HPQCD, blue FNAL-MILC) and ‘experimental’ points (black triangles, upward-pointing for tagged and downward pointing for untagged data) constructed by plotting at the centre of each bin the constant form factor that would reproduce the partial branching fraction in that bin. The top right plot shows the differential decay rate together with the experimental inputs. The bottom plots provide more details of the inputs and fits by showing on the left  $\log[(m_{B^*}^2 - q^2)f_+(q^2)/m_{B^*}^2]$  as a function of  $q^2$ , and on the right  $P\phi f_+$  as a function of  $-z$ . The dashed magenta curve in the bottom right plot is a cubic polynomial fit in  $z$  to the Omnès curve.

- Since we do not know the correlations between the lattice input data we have also performed a fit neglecting all correlations in these inputs. We find that  $|V_{ub}|$  increases by an amount  $0.18 \times 10^{-3}$ , which we will quote as a systematic error in our determination. We observe that knowledge of the correlations will be needed for more precise determinations of  $|V_{ub}|$ .
- The inclusion of  $f_0$  in the analysis has no visible effect in our results for  $f_+$  and  $|V_{ub}|$ . This is not surprising given that the number of input data affecting  $f_+$  is much bigger than that affecting  $f_0$  and that the parametrisation allows the data to determine each form factor independently apart from the constraint at  $q^2 = 0$ . The covariance matrix given in appendix B shows this freedom, having negligible correlations between  $f_+$  and  $f_0$  at  $q^2 \neq 0$ . Correlations linking  $f_+$  and  $f_0$  in the lattice QCD inputs could modify the central values in (9) by an amount comparable to their errors as we have confirmed by fully-correlating the systematic errors between them. As an example, for  $|V_{ub}|$  we find a central value of  $4.15 \times 10^{-3}$ . Since we do not know the actual correlation information<sup>2</sup> for the lattice data, we do not present

<sup>2</sup>It is reasonable to expect correlations not only in the systematic error but also in the statistical ones, since  $f_+$  and

these numbers.

- Because of the freedom allowed by the Omnès parametrisation of  $f_+$  and  $f_0$ , one may wonder whether or not heavy quark symmetry (HQS) relations between the form factors at  $q_{\max}^2$  are satisfied. Some earlier parametrisations were explicitly constructed to satisfy the HQS scaling relation  $f_+(q_{\max}^2)/f_0(q_{\max}^2) \sim m_B$ , for example dipole/pole forms [27–29], and these have been widely used. From our fit we calculate

$$\frac{1}{m_B} \left. \frac{f_+(q_{\max}^2)}{f_0(q_{\max}^2)} \right|_{B\pi} = 1.3 \pm 0.4 \text{ GeV}^{-1} \quad (10)$$

to be compared to the corresponding quantity in  $D \rightarrow \pi$  exclusive semileptonic decays,  $1.4 \pm 0.1 \text{ GeV}^{-1}$  extracted from the unquenched lattice QCD results in [30]. This agreement is reassuring but our determination of the ratio in  $B \rightarrow \pi$  decays has a further uncertainty of around 10% arising from our incomplete knowledge of the correlations in the lattice inputs.

- Heavy quark effective theory in the soft-pion limit predicts [31],

$$f_0(m_B^2) = f_B/f_\pi + \mathcal{O}(1/m_b^2) \approx 1.4(2) \quad (11)$$

where we have used  $f_B = 189(27) \text{ MeV}$  [32]. Our fit for  $f_0(q_{\max}^2)$  in equation (9) is compatible within errors.

- Applying soft collinear effective theory (SCET) to  $B \rightarrow \pi\pi$  decays allows a factorisation result to be derived which leads to a model-independent extraction of the form factor (multiplied by  $|V_{ub}|$ ) at  $q^2 = 0$  [33]. We quote the result from our fit,

$$|V_{ub}|f^+(0) = (8.8 \pm 0.8) \times 10^{-4}, \quad (12)$$

which compares well with  $|V_{ub}|f^+(0) = (7.6 \pm 1.9) \times 10^{-4}$  quoted in [17]. This also agrees with the value  $|V_{ub}|f^+(0) = (9.1 \pm 0.7) \times 10^{-4}$  [19] obtained by fixing  $|V_{ub}|$  from global CKM unitarity triangle fits and fitting to the BaBar 12-bin data [23].

- We noted above possible effects of correlations in the lattice data. Other sources of systematic variation in the result for  $|V_{ub}|$  arising from uncertainties in the theoretical form factor inputs at or near  $q^2 = 0$  were considered in [18] and shown to be safely covered by the statistical uncertainty.

## 4 Conclusion

We have updated our previous analysis of exclusive  $B \rightarrow \pi$  semileptonic decays, based on Omnès dispersion relations. The principal change is to improve the treatment of the  $B^*$  and its effect on the form factor  $f_+$ . We have also incorporated the scalar form factor  $f_0$  in a simultaneous analysis and examined the possible effects of correlations among lattice inputs. Finally, we have taken advantage of new experimental data from the BaBar 12-bin untagged analysis [6]. We extract a value

$$|V_{ub}| = (3.90 \pm 0.32 \pm 0.18) \times 10^{-3}. \quad (13)$$

---

$f_0$  are linear combinations of temporal and spatial components of vector current matrix elements.

The first error above is statistical arising from the chi-squared fit. The second is a systematic error to account for current partial knowledge of correlations in the lattice input data. The precision for  $|V_{ub}|$  is comparable with that of the inclusive determination and we do not find a significant discrepancy between our result and the inclusive world average value,  $(4.45 \pm 0.20 \pm 0.26) \times 10^{-3}$  [1].

Finally we would like to stress that the Omnès parametrisation is physically motivated and simple and provides a robust framework for a precise exclusive determination of  $|V_{ub}|$ .

## Acknowledgements

JMF acknowledges the hospitality of the Departamento de Física Atómica, Molecular y Nuclear, Universidad de Granada, MEC support for estancias de Profesores e investigadores extranjeros en régimen de año sabático en España SAB2005–0163, and PPARC grant PP/D000211/1. JN acknowledges support from Junta de Andalucía grant FQM0225 and MEC grant FIS2005–00810. JMF and JN acknowledge support from the EU Human Resources and Mobility Activity, FLAVIANet, contract number MRTN–CT–2006–035482.

## A Choice of $\delta_{IJ}(s_{\text{th}})$ in the Omnès Representation

In this appendix we provide more details on some aspects of the Omnès representation of the form factors. This builds on the discussion in the appendix of [34].

The scattering matrix  $T$  depends on  $\exp(2i\delta)$  and thus one has the freedom to add factors of  $k\pi$  to the phase shift, for integer  $k$ , without modifying the  $T$  matrix. However, the Omnès representation of the form factor certainly depends on the specific value of  $k$ . Indeed adding  $k\pi$  to  $\delta$  leads to

$$\exp \left\{ I_{\delta+k\pi} \times \prod_{j=0}^n (q^2 - s_j) \right\} = \exp \left\{ I_{\delta} \times \prod_{j=0}^n (q^2 - s_j) \right\} \left( \frac{\prod_{j=0}^n (s_{\text{th}} - s_j)^{\alpha_j(q^2)}}{s_{\text{th}} - q^2} \right)^k \quad (14)$$

which induces an unphysical  $k$ th order pole in the form factor at  $s_{\text{th}}$ .

Now consider  $\mathcal{F}(q^2) = (m_{B^*}^2 - q^2)f_+(q^2)$ , which has no poles in  $0 \leq q^2 \leq s_{\text{th}}$ . Its Omnès representation should not induce a pole at  $s_{\text{th}}$  and therefore we should set  $k = 0$  in equation (14) above. This is equivalent to setting  $\delta_{1/2,1}(s_{\text{th}}) = 0$ . With enough subtractions, we can then take  $\delta_{1/2,1}(s) = 0$  inside the integral because only the region close to  $s_{\text{th}}$  will be important, leading to the result presented in equation (7).

This choice for  $\delta_{1/2,1}(s_{\text{th}})$  does not contradict Levinson's theorem, which fixes only the difference

$$\delta_{1/2,1}(\infty) - \delta_{1/2,1}(s_{\text{th}}) = \pi(n_z - n_p) \quad (15)$$

where  $n_z$  ( $n_p$ ) is the number of zeros (poles) of the scattering matrix  $T$  on the physical sheet. The usual convention [35] is to set  $\delta_{1/2,1}(s_{\text{th}}) = \pi n_p$  and  $\delta_{1/2,1}(\infty) = \pi n_z$ . However, we use a different convention which follows from the discussion above on the effect of adding multiples of  $\pi$  to the phase shift. Our choice is  $\delta_{1/2,1}(s_{\text{th}}) = 0$  which therefore also implies that  $\delta_{1/2,1}(\infty) = 0$ .

In our previous work [18, 20, 34], we assumed that  $f_+$  had no poles. With the usual convention for Levinson's theorem that  $\delta_{1/2,1}(s_{\text{th}}) = \pi$ , we developed a pole for  $f_+$  at  $s_{\text{th}}$  which was not discarded since it mimicked the  $B^*$  pole's effects on the form factor because  $m_{B^*}^2 \approx s_{\text{th}}$ . We already commented on this in the appendix of [34].

## B Correlation Matrix

Here we give the correlation matrix of fitted parameters corresponding to the best-fit parameters in equation (9).

$$\begin{pmatrix} 1 & -0.43 & -0.91 & -0.81 & -0.58 & -0.04 & 0.00 & 0.01 \\ & 1 & 0.20 & 0.50 & -0.04 & 0.10 & 0.00 & -0.02 \\ & & 1 & 0.76 & 0.61 & 0.02 & 0.00 & 0.00 \\ & & & 1 & 0.36 & 0.05 & 0.00 & -0.01 \\ & & & & 1 & 0.00 & 0.00 & 0.00 \\ & & & & & 1 & 0.32 & 0.83 \\ & & & & & & 1 & 0.22 \\ & & & & & & & 1 \end{pmatrix} \quad (16)$$

## References

- [1] Heavy Flavor Averaging Group (HFAG) (2006), hep-ex/0603003.
- [2] CLEO Collaboration, S.B. Athar et al., Phys. Rev. D68 (2003) 072003, hep-ex/0304019.
- [3] Belle Collaboration, T. Hokuue et al. (2006), hep-ex/0604024.
- [4] BABAR Collaboration, B. Aubert et al., Phys. Rev. D72 (2005) 051102, hep-ex/0507003.
- [5] BABAR Collaboration, B. Aubert (2006), hep-ex/0607089.
- [6] BABAR Collaboration, B. Aubert et al., Phys. Rev. Lett. 98 (2007) 091801, hep-ex/0612020.
- [7] E. Dalgic et al., Phys. Rev. D73 (2006) 074502, hep-lat/0601021.
- [8] M. Okamoto et al., Nucl. Phys. Proc. Suppl. 140 (2005) 461, hep-lat/0409116.
- [9] M. Okamoto, PoS LAT2005 (2006) 013, hep-lat/0510113.
- [10] Fermilab Lattice, MILC and HPQCD Collaboration, P.B. Mackenzie et al., PoS LAT2005 (2006) 207.
- [11] R.S. Van de Water and P. Mackenzie, PoS LAT2006 (2006) 097.
- [12] P. Ball and R. Zwicky, Phys. Rev. D71 (2005) 014015, hep-ph/0406232.
- [13] L. Lellouch, Nucl. Phys. B479 (1996) 353, hep-ph/9509358.
- [14] G. Burdman and J. Kambor, Phys. Rev. D55 (1997) 2817, hep-ph/9602353.
- [15] M. Fukunaga and T. Onogi, Phys. Rev. D71 (2005) 034506, hep-lat/0408037.
- [16] M.C. Arnesen, B. Grinstein, I.Z. Rothstein and I.W. Stewart, Phys. Rev. Lett. 95 (2005) 071802, hep-ph/0504209.
- [17] I.W. Stewart, in CKM2006, 4th Int. Wkshp. on the CKM Unitarity Triangle, Nagoya, Japan, 12–16 Dec 2006 (2006) .

- [18] J.M. Flynn and J. Nieves, Phys. Rev. D75 (2007) 013008, hep-ph/0607258.
- [19] P. Ball, Phys. Lett. B644 (2007) 38, hep-ph/0611108.
- [20] J.M. Flynn and J. Nieves, Phys. Lett. B505 (2001) 82, hep-ph/0007263.
- [21] R. Omnes, Nuovo Cim. 8 (1958) 316.
- [22] N.I. Mushkelishvili, Singular Integral Equations (Noordhoff, Groningen, The Netherlands, 1953).
- [23] BABAR Collaboration, B. Aubert et al. (2006), hep-ex/0607060.
- [24] K.M. Watson, Phys. Rev. 95 (1954) 228.
- [25] J.M. Flynn and J. Nieves, Phys. Rev. D75 (2007) 074024, hep-ph/0703047.
- [26] BABAR Collaboration, B. Aubert et al. (2006), EPAPS database entry E-PRLTAO-98-086710, <http://www.aip.org/pubservs/epaps.html>.
- [27] UKQCD Collaboration, D.R. Burford et al., Nucl. Phys. B447 (1995) 425, hep-lat/9503002.
- [28] UKQCD Collaboration, L. Del Debbio, J.M. Flynn, L. Lellouch and J. Nieves, Phys. Lett. B416 (1998) 392, hep-lat/9708008.
- [29] D. Becirevic and A.B. Kaidalov, Phys. Lett. B478 (2000) 417, hep-ph/9904490.
- [30] Fermilab Lattice Collaboration, C. Aubin et al., Phys. Rev. Lett. 94 (2005) 011601, hep-ph/0408306.
- [31] G. Burdman, Z. Ligeti, M. Neubert and Y. Nir, Phys. Rev. D49 (1994) 2331, hep-ph/9309272.
- [32] S. Hashimoto, Int. J. Mod. Phys. A20 (2005) 5133, hep-ph/0411126.
- [33] C.W. Bauer, D. Pirjol, I.Z. Rothstein and I.W. Stewart, Phys. Rev. D70 (2004) 054015, hep-ph/0401188.
- [34] C. Albertus et al., Phys. Rev. D72 (2005) 033002, hep-ph/0506048.
- [35] A.D. Martin and T.D. Spearman, Elementary Particle Theory (North Holland, Amsterdam, 1970) p. 401.